Optical Tweezers and Brownian Motion

Adam Pearl[1, *] and Nicholas Lyu[1, †]

[1] *Department of Physics, Harvard University, Cambridge, Massachusetts 02138, USA*

(Dated: February 27, 2025)

We assembled an optical tweezer using an inverted what? microscope objective and a Hitachi HL6501MG 658nm laser diode. Using the tweezer, we demonstrate 3D trapping of 5μm microspheres in aqueous solutions and measured the trap depth of the tweezer as a function of different laser powers. Additionally, using a custom algorithm for determining the spheres' locations on various frames, we analyzed the Brownian motion of microspheres and experimentally determined the Boltzmann constant to be $x \pm y\,\mathrm{J/K}$, a how much over/under-estimate compared to the established value $1.381 \cdot 10^{-23}\,\mathrm{J\,K^{-1}}$.

I. INTRODUCTION

Optical tweezers use a tightly focused laser beam to trap microscopic systems by electromagnetic gradient forces [1, 2]. They constitute a powerful tool for manipulating microscopic and many-body quantum systems [3, 4]. In this experiment, we built a basic optical tweezer and imaging system analogous to the design outlined in in [2]. We demonstrate trapping dielectric microbeads in an aqueous solution, and measure the trap depth at different laser powers. By analyzing the bead motion using a custom video capture algorithm, we analyze the Brownian motion of the microspheres to experimentally determine the Boltzmann constant using calculations outlined in [5].

Paragraph roughly describing the physical mechanism of optical tweezers; relate to citations Two main models describe forces in optical traps [1, 2]:

- **Ray Optics:** Momentum changes of refracted beams produce net restoring forces toward the focal spot. A collimated laser beam incident on a sphere will undergo both reflection and refraction. Each change in the direction of the beam imparts momentum on the sphere. Whether the sphere is centered above or below the focal point, the net force is towards the focus of the laser more on this with figure.[6]
- **Dipole Approximation:** The induced dipole moment interacts with the field gradient.

With a proper focus and high enough laser power, a large gradient force can overcome thermal motion to confine particles in three dimensions.

We measure trap depth by observing the period it takes for a particle to escape a trap, from which we can then obtain the maximum velocity at which a translating sample can hold a bead in the trap (the "escape velocity"). More details on the physics of optical tweezers. Reference [2]. Sensitivity to changes in depth

Paragraph roughly describing the physics of Brownian motion, Stokes drag, and Boltzmann constant

II. EXPERIMENTAL SETUP

A. Trapping and Imaging systems

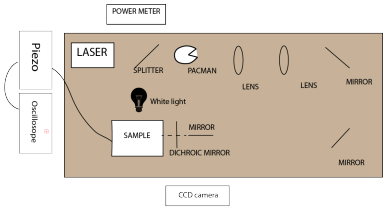

FIG. 1. Schematic of table set up

We followed the circuit in [7] to shape the intial 658nm beam from a Hitachi HL6501MG laser diode. The fiber-coupled initial laser is extracted and passed through a magnification telescope consisting of convex focal lengths lenses. The resulting beam is passed to an inverted microscope design to match the measured microscope objective diameter of 6mm. The optical table layout is depicted in Fig 1.

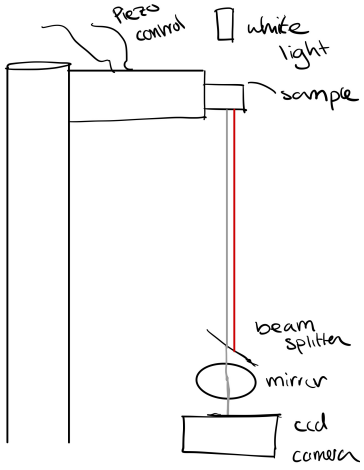

FIG. 2. (placeholder) Tweezer and imaging system.

The tweezer system (Fig 2) consists of a exact model

* apearl@college.harvard.edu
† nicholaslyu@college.harvard.edu

dichroic mirror which selectively reflects 658nm light, an inverted, collimated microscope objective with 100 times magnification, and a model optical translation stage with piezo control. The incoming trapping beam is reflected by the dichroic mirror and focused by the microscope objective onto the sample. A separate white-light illumination provided on the opposite direction of the sample passes through the dichroic mirror and is focused on a Thorlabs model camera, resulting in video imaging with a blue background. Compared to [7] and [2], the objective of the microscope in our setup expects collimated beams; this allows us to omit a substantial portion of beam-shaping circuits. The camera imaging circuit involves a 50mm focusing lens and model camera directed at the microscope objective. Since both involve collimated light, focal plane of the camera roughly coincides with that for the trapping beam, so we expect sharp imaging of the trapped particles.

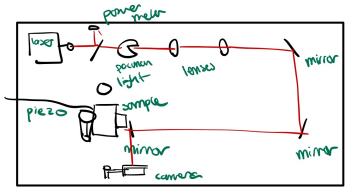

FIG. 3. Airy disc pattern of the trapping beam

The magnified trap beam is highly symmetric. However, we identified an Airy disc pattern (Fig 3) which deviate from the expected fundamental Gaussian mode. We haven't been able to visually identify this pattern from the fiber-coupled output prior to telescoping, which suggests that the diffraction pattern could be due to us using small, exact-size, half-inch? lenses for magnification. It is also possible that the fiber-coupled output already contains higher-order modes prior to telescoping; the exact identification of the source of the diffraction pattern requires a beam camera.

B. Sample Preparation and Trap Calibration

Include sample schematic

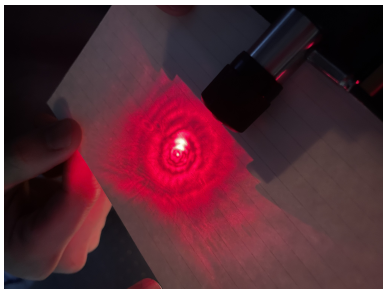

FIG. 4. Diffraction pattern of a stably trapped microsphere.

We use a 2:1000 edit accordingly sample of polystyrene microspheres in de-ionized water. We repeated the experiment both with $3\mu m$ and $30\mu m$ edit accordingly spheres.

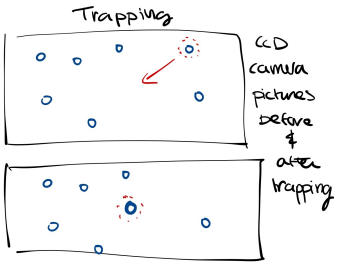

FIG. 5. CCD capture of particle being trapped

The telescoping circuit is aligned with standard techniques; the beam is kept at a constant height and parallel to the breadboard axes. We align the vertical entry of the trap beam by adjusting the dicroic mirror to center the diffracted pattern on the sample site; this centers the x-y dimension of our tweezer. The calibration of the z-axis proceeds in three steps:

1. To obtain the coarsest alignment, we load a sample and inspect the trapping beam's diffraction pattern through the sample. The microspheres appear as concentric circles with increasing diameter as it nears the focus of the trapping beam. At a suitable coarse range of height, we observe large (in-focus) microsphere patterns suddenly attracted into the center then decrease in size as they escape along the z-axis.
2. We next fine-adjust the z-translation to ensure that the microspheres are subject to stable 3D trapping. This is done by adjusting the z-axis until the trapped diffraction patterns remain stable (Fig 4).
3. To fine-tune the trap, we image the trap (Figure 5) and turn on the PZT to induce circular motion of the samples. For each z-displacement, we identify the maximum frequency at which the microsphere remains trapped and optimizes this frequency.

C. Measuring Trap Depth

The main objective of this experiment is to measure the trap depth as a function of laser power. In our optical tweezer experiment, we measure the piezo driving frequency at which a particle caught in a trap escapes the trap as a function of laser power. In order to extract from these measurements a relationship between laser power and trap depth, we need to make some conversions. The path a particle follows is determined by the piezo sine and cosine diving frequency.

$$\boldsymbol{x}(t) = (A\cos(2\pi t/\tau), A\sin(2\pi t/\tau))$$

And has a linear velocity of $v = \frac{2\pi A}{\tau}$, so $v_{\text{esc}} = \frac{2\pi A}{\tau_{\text{esc}}}$

The trap depth represents the binding energy of the trap, $D = F_{\max} w_{\text{trap}}$. The maximum restoring force on the bead from the trap is infered from the escape velocity, whereas the trap width is characteristics of the laser and beads.

In order for the trap to retain a bead it must provide a restoring force greater than or equal to the stokes drag caused by the solution moving relative to the bead given by $F_S = 6\pi\eta r v$ where η is the viscosity of the solution ($10^{-3} Ns/m^2$ for water). Therefore $F_{\max} = 6\pi\eta r v_{\text{esc}}$. From [REF], an ideal lens with numerical aperture NA, passing through a medium with index of refraction n, focusing a collimated laser with wavelength λ will produce a trap of width

$$w_{\text{trap}} \geq \frac{1.22\lambda}{n}\sqrt{\left(\frac{n}{\text{NA}}\right)^2 - 1}$$

and therefore (assuming ideal lens?)

$$D = \frac{6.32\pi\eta r v_{\text{esc}}\lambda}{n}\sqrt{\left(\frac{n}{\text{NA}}\right)^2 - 1}$$

The multiplicative error is

$$\sigma_D^2 = D^2\left(\frac{\sigma_\eta^2}{\eta^2} + \frac{\sigma_r^2}{r^2} + \frac{\sigma_{v_{\max}}^2}{v_{\max}^2}\right)$$

III. BOLTZMANN CONSTANT MEASUREMENT

A. Particle tracking

The video camera provides real-time videos of microspheres in the focal plane. The camera input is monitored using the ThorCams software; since ThorCams does not offer native video capture, we use a third-party screen-capture software to save the videos. We use a custom microsphere tracking algorithm to extract the center of microspheres within each frame. Specification of the processing algorithm, its inputs and outputs. The microsphere tracking algorithm outputs the pixel location of the microspheres as a function of time; the next section details how pixel information is converted into physical length.

B. Boltzmann's Constant Estimation

Assuming Brownian motion data $(x_j(t), y_j(t))_{j=1,\dots N}$ of N particles for $t = t_1, \dots, t_m$, where x_t, y_t are the displacement of the particles from their original position, we can estimate the mean-squared displacement of the particles as a function of time.

$$\langle R\rangle_t = \frac{1}{N}\sum_{j=1}^{N} x_j(t)^2 + y_j(t)^2. \tag{1}$$

The measured two-dimensional mean-squared displacement is proportional to the drift time and Boltzmann constant via [see 5, Eq. 3]

$$\langle R^2(t)\rangle = \frac{4k_B T}{6\pi\eta a}t \iff \hat{k}_B = \frac{6\pi\eta a}{4T}\cdot\frac{\widehat{\langle R^2(t)\rangle}}{t} \tag{2}$$

here k_B is the Boltzmann constant, T is the temperature, η is the viscosity of the solution, and a is the spherical particle's radius. The ensemble-average formula is derived by solving for the equilibrium mean squared displacement as a function of a dissipative drag force, which can be determined using Stokes' law and the viscosity. Error sources include the temperature σ_T, viscosity σ_η, diameter σ_a, as well as the linear fit error σ_β.

IV. EXPERIMENTAL RESULTS

We collect the following data:

- 30 videos of 30s particle drifts, for 5μm spheres in 2 : 1000 sample of de-ionized water.
- For laser-driving current $I_{\text{LD}} \in \{80, 85, 90, 95\}$ mA, the maximum PZT oscillation frequency at which microspheres remain trapped.

A. Trap depth measurement

In order to measure τ_{esc}, we first trap a sphere with the piezo turned off. We then initiate the piezo and calibrate the trap such that it can hold the sphere at the minimum possible driving period. At each recorded value of power, we measure the minimum driving period at which the particle remains in the trap. Upon doing initial trials, we realized that $P - D$ curves were offset from trial to trial. This is likely because our trap was sensitive to distance and fell out of calibration over time. We corrected this by recalibrating the trap at the beginning of every trial.we need to figure out how to avoid de-callibration within each trial.

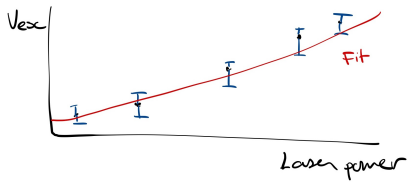

FIG. 6. Escape velocity vs laser power (data pending)

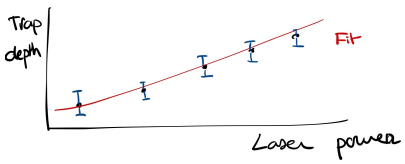

FIG. 7. Trap depth vs laser power (data pending)

Verbal explanation of the results, and comparison to what we would expect. Discussion of possible differences between 3-micrometer and 30-micrometer measurements.

B. Boltzmann constant estimate

Based on the 30 videos, we have been able to consistently track the displacements of N =? particles (Figure 8). calculations. Explanation of the fit results; comparison to the true Boltzmann constant, and discussion for potential sources and propagation of errors.

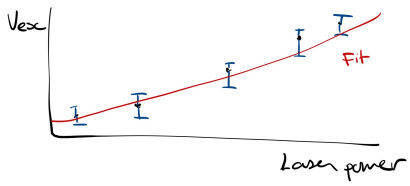

FIG. 8. Centered displacement behavior of the tracked microsphere ensemble.

From equation 2, we expect the observed expected mean-squared displacement $\langle R^2(t)\rangle$ to be a linear function of t. We estimate the slope $\beta = \langle R^2(t)\rangle/t$ using a univariate linear regression through the origin [8]: given $(t_j, \langle R^2(t_j)\rangle)_{j=1}^N$, the point estimate is

$$\hat{\beta} = \frac{\sum_{j=1}^N t_j \langle R^2(t_j)\rangle}{\sum_{j=1}^N t_j^2} \tag{3}$$

The unbiased estimate of the residual standard deviation and the slope's error are, correspondingly,

$$\hat{\sigma}^2 = \frac{1}{n-1}\sum_{j=1}^N \left[\langle R^2(t_j)\rangle - \hat{\beta} t_j\right]^2, \quad \hat{\sigma}_\beta = \frac{\hat{\sigma}}{\sqrt{\sum_{j=1}^N t_j^2}} \tag{4}$$

However, we note that the formula above assumes homoskedasticity, i.e. the variance of $\langle R^2(t)\rangle$ is constant with respect to t. In practice, we observe that the variance of$\langle R^2(t)\rangle$ increases with t (Figure 9), violating the homoskedasticity assumption. To account for this, we use the heteroskedasticity-consistent estimate of β's standard error, given by

$$\hat{\sigma}_\beta = \frac{\sqrt{\sum_{j=1}^N t_j^2 \left[\langle R^2(t_j)\rangle - \hat{\beta} t_j\right]^2}}{\sum_{j=1}^N t_j^2} \tag{5}$$

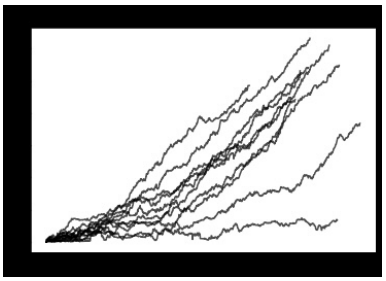

FIG. 9. Displacement vs time for the tracked particles. Notice that the variance of the displacement increases with time.

Use the heteroskedasticity-consistent estimate of β's standard error. Further recall that given $k_B = f(\eta(T), T, a, \beta)$ as in equation 2, the error formula is

$$\begin{aligned}\sigma_{\hat{k}_B}^2 &= \left(\sigma_T \frac{df}{dT}\right)^2 + (\sigma_a \partial_a f)^2 + (\sigma_\beta \partial_\beta f)^2 \\ &= \frac{9\pi^2}{4T^2}\left[\beta^2\sigma_a^2\eta^2 + a^2\sigma_\beta^2\eta^2 + \sigma_T^2 a^2\beta^2\left(\eta'(T) - \frac{\eta}{T}\right)^2\right]\end{aligned} \tag{6}$$

The temperature measures to to 20.3 ± 0.1°C. To obtain the viscosity, we used a reviewed online viscosity calculator to obtain the viscosity point-estimates around 20.3°C.

$$\eta \begin{pmatrix} 20.2 \\ 20.3 \\ 20.4 \end{pmatrix} °\mathrm{C} = \begin{pmatrix} 0.9968 \\ 0.9944 \\ 0.992 \end{pmatrix} \mathrm{mPa \cdot s}$$

Using these estimates, we estimate the viscosity derivative using central difference:

$$\eta'(20.3\,°\mathrm{C}) \approx \frac{\eta(20.4\,°\mathrm{C}) - \eta(20.2\,°\mathrm{C})}{0.2\,°\mathrm{C}} = -0.024\,\mathrm{mPa \cdot s/°C} \tag{7}$$

Our estimates of these values are

$$\hat{\beta} = 1\mathrm{m}^2/\mathrm{s}, \quad \hat{\sigma} = 1\mathrm{m}^2, \quad \hat{\sigma}_\beta = 1\mathrm{m}^2/\mathrm{s} \tag{8}$$

$$\hat{\sigma}_{k_B} = x\mathrm{J}^2/\mathrm{K} \tag{9}$$

V. DISCUSSION

Summary of our findings and deviation from theoretically expected results; discuss how the measured k_B deviates from the expected k_B, whether it is in-range, and if not, potential sources of systematic bias. Discussion of overall areas for improvement and sources of error. Ideas for future, more advanced versions of this experiment

ACKNOWLEDGMENTS

The authors thank the teaching staff of Physics 191 for providing invaluable help in the assembly and calibration of this experiment: Jieping Fang, Joe Peidle, Jenny Hoffmann, and Philip Kim. Author NL wrote the abstract, optical setup, imaging, trap calibration, and Brownian motion analysis. Author AP documented the sample preparation, trap depth calculation, and figures. Both authors contributed to the introduction. acknowledgement for discussion and data analytics.

[1] A. Ashkin, J. M. Dziedzic, J. E. Bjorkholm, and S. Chu, Optics Letters **11**, 288 (1986).
[2] S. P. Smith *et al.*, American Journal of Physics **67**, 26 (1999).
[3] D. Bluvstein, H. Levine, G. Semeghini, T. T. Wang, S. Ebadi, M. Kalinowski, A. Keesling, N. Maskara, H. Pichler, M. Greiner, *et al.*, Nature **604**, 451 (2022).
[4] J. Beugnon, C. Tuchendler, H. Marion, A. Gaëtan, Y. Miroshnychenko, Y. R. Sortais, A. M. Lance, M. P. Jones, G. Messin, A. Browaeys, *et al.*, Nature Physics **3**, 696 (2007).
[5] P. Nakroshis, M. Amoroso, J. Legere, and C. Smith, American Journal of Physics **71**, 568 (2003).
[6] T. A. Nieminen, N. Du Preez-Wilkinson, A. B. Stilgoe, V. L. Loke, A. A. Bui, and H. Rubinsztein-Dunlop, Journal of Quantitative Spectroscopy and Radiative Transfer **146**, 59 (2014).
[7] M. Prentiss, Optical and magnetic tweezers: Advanced physics laboratory, Harvard Wiki (2003).
[8] J. K. Blitzstein and N. Shephard, *Stat 111: Introduction to Statistical Inference* (Self-published, 2024) ©2023 by Joseph K. Blitzstein and Neil Shephard.